Supplemental Material

Materials & Methods: blood clot samples

After local institutional review board approval and informed written consent, venous whole blood was drawn from patients undergoing invasive catheterization procedures at the University of Chicago Medicine cardiac catheterization laboratory. Following an established protocol (Sutton *et al* 2013, Mercado-Shekhar *et al* 2018), in vitro clots were then produced in Pasteur pipettes (14.6 cm length, 2 mL capacity, Fisher Scientific, Hanover Park, IL, USA). Clots were approximately 4 mm in diameter. The clots were removed from the pipettes by gently flushing with isotonic saline (0.9% NaCl w/v), and suspended in the acrylic mold with nylon thread. An isotonic (0.9% NaCl w/v) low-gelling temperature liquid agarose mixture (2% w/v, product number A0701, Sigma-Aldrich, St. Louis, MO, USA) was cooled to 40°C and poured into the mold. The agarose was allowed to solidify, after which the agarose-embedded clot was stored at 4°C overnight. A total of 4,000 pulses with a peak negative pressure of 18 MPa were generated in three locations in each of three clots (nine total data sets). Passive cavitation and plane wave images were acquired during insonation as described in the main text. MR imaging parameters for diffusion imaging of clot samples are listed in Table S1. All other post-hoc MR and conventional B-mode images of insonated clot samples were acquired as described in the main text. Four-millimeter sections encompassing the liquefied regions were collected from each insonified region of the clot samples. These samples were processed and stained with H&E as described in the main text. Registration between imaging and histological clot samples was not possible due to movement of residual clot during fixing and processing. Minimal changes in tissue sample size and shape occurred due to histological processing. Background ROIs were

drawn for each sample in untargeted portions of clots, and the average PCI acoustic power, plane wave and post hoc conventional B-mode grayscale, T_1, T_2, and ADC values within the liquefaction zones and background ROIs were computed. Differences in these values were evaluated for significance as described in the main text.

Table S1: MR scan parameters used for parametric mapping of ADC in blood clot samples.

Sequence	TR/TE (ms)	In-plane resolution (acquisition) (mm^2)	Array size (recon matrix)	Slice thickness (mm)	NSA	Echo factor	TI (ms)	b-values (s/mm^2)
ADC mapping for blood clot samples (DWI TSE)	5000/73	1.5 x 1.5	384 x 384	3	6	65 (TSE)	N/A	0, 500, 1000

TR/TE = repetition time/echo time; NSA = number of signal averages; TI = inversion time; TSE = turbo spin echo; ADC = apparent diffusion coefficient; DWI = diffusion-weighted imaging.

Results: blood clot samples

Table S2 displays bubble-monitoring and post-insonation image parameter values measured within liquefaction zones for clot samples. Histotripsy-induced clot liquefaction significantly increased T_1, T_2, and ADC by 302 ± 122 ms, 35 ± 8 ms, and 0.48 ± 0.11 mm^2/ms, respectively, compared with untreated clot areas. The maximal increases in T_2 coincided with clot/agarose interfaces, likely due to magnetic susceptibility effects (Figure S1). Regions of clot liquefaction exhibited uniform increases in T_1 and ADC relative to areas of untreated clot. The strongest acoustic emissions in clot samples were in the center of the liquefaction zone, with weaker emissions on either side of this location. Previous studies have demonstrated a threshold acoustic emission power required for liquefaction that may be considerably lower than the peak emissions observed (Bader *et al* 2018). It is therefore not surprising that liquefaction was observed

throughout most of the azimuthal extent of the clot despite a large variation in acoustic emission power along this dimension (Figure S1).

Table S2: Diagnostic ultrasound and MR parameter values measured within liquefaction zones for clot samples insonated at 18 MPa.

Bubble activity monitoring	
PCI Acoustic Power ($\times 10^5$ *V*^{2})	2.01 ± 0.46*
Plane Wave Grayscale ($\times 10^8$)	5.25 ± 1.06*
Post-hoc evaluation	
Post-hoc conventional B-mode Grayscale ($\times 10^8$)	30.6 ± 15.9*
T_1 *(ms)*	1240 ± 152*
T_2 *(ms)*	107 ± 20*
ADC (*mm*^{2}*/ms*)	1.13 ± 0.08*

* Liquefaction zone significantly different from background (untreated) clot.
All errors are given as standard deviations.

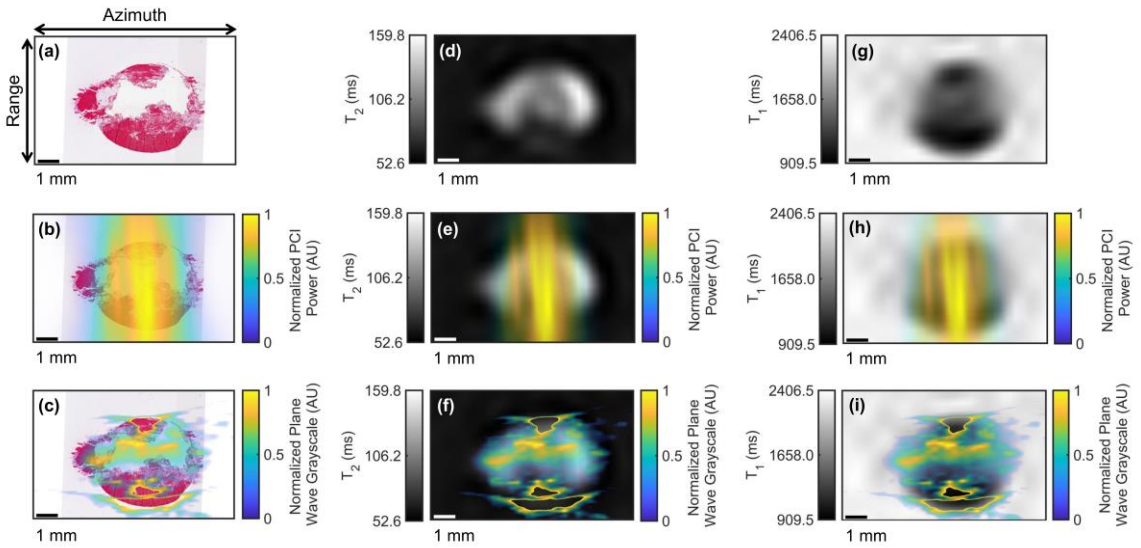

Figure S1: Registration of imaging with histologic observation of blood clot sample liquefaction. (a) Hematoxylin and eosin (H&E) stain of blood clot sample exposed to histotripsy, (b) coregistration of passive cavitation imaging (PCI) acoustic power and H&E-stained clot sample, (c) coregistration of plane wave grayscale and H&E-stained clot sample, (d) parametric T_2 map of treated clot sample, (e) coregistration of PCI acoustic power and T_2 map, (f) coregistration of plane wave grayscale and T_2 map, (g) parametric T_1 map of treated clot sample, (h) coregistration of PCI acoustic power and T_1 map, and (i) coregistration of plane wave grayscale and T_1 map. The histotripsy pulse (1-MHz fundamental frequency, 5-µs pulse duration, 18-MPa peak negative pressure) propagated from left to right in the image. The azimuth/range dimensions of the diagnostic ultrasound imaging plane are indicated in the panel (a). The most hyperechoic pixels in the plane wave images, corresponding to reflections from the top and bottom of the clot, have been removed for better windowing and visualization of the histotripsy bubble cloud.

Supplemental data for RBC phantoms and liver samples

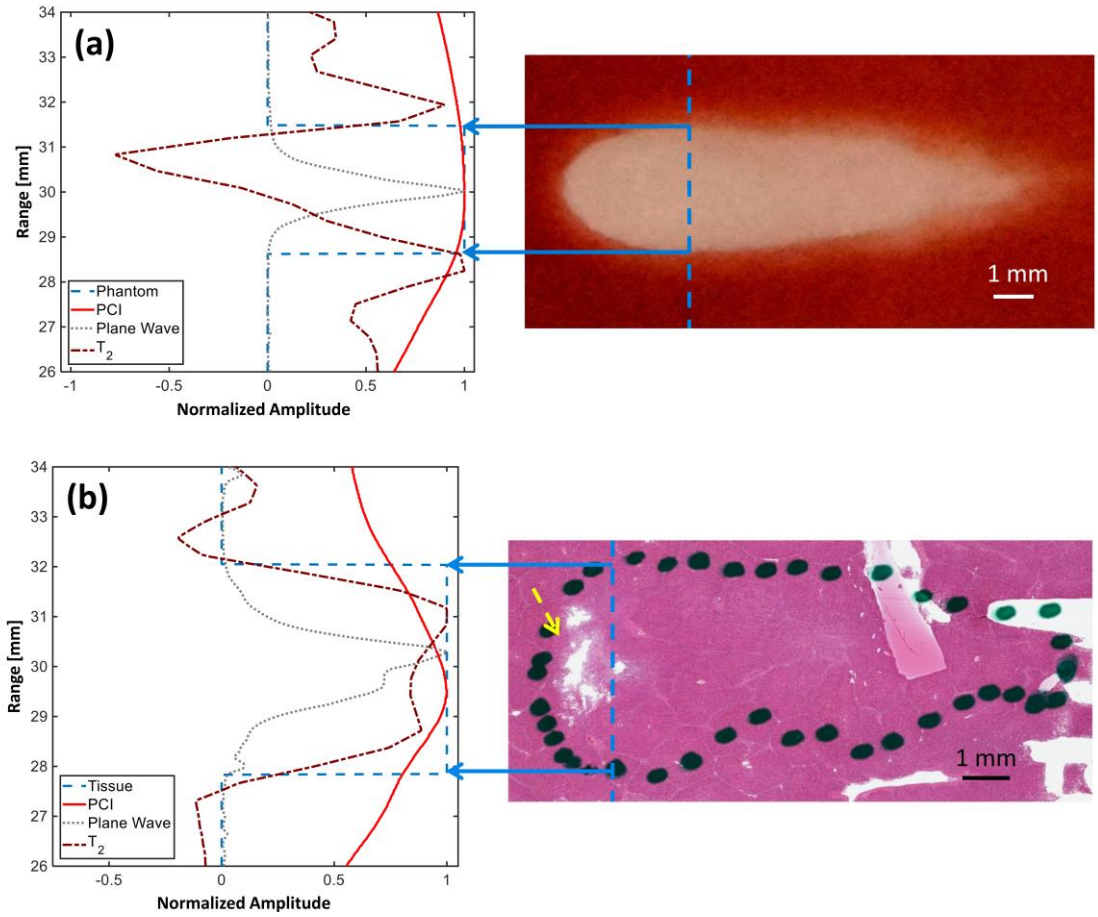

Figure S2: Normalized amplitudes of passive cavitation imaging (PCI) acoustic power, plane wave grayscale, and change in T_2 from background at the azimuth position of maximum PCI power (vertical dashed blue lines in right-side images) for (a) a red blood cell phantom, and (b) a liver sample. Apparent diffusion coefficient signals in red blood cell phantoms and T_1 and plane wave grayscale signals in all samples were dominated by noise and thus excluded from this figure. The locations of liquefaction are binarized for the plots, with values of 1 indicating liquefaction and 0 indicating intact media. The azimuthal location of maximum PCI power in the liver sample corresponds with more thorough liquefaction as indicated by hematoxylin and eosin staining (yellow dashed arrow). The histotripsy pulse (1-MHz fundamental frequency, 5-μs pulse duration, 17-MPa peak negative pressure for RBC phantom, 25-MPa peak negative pressure for liver sample) propagated from left to right in each image.

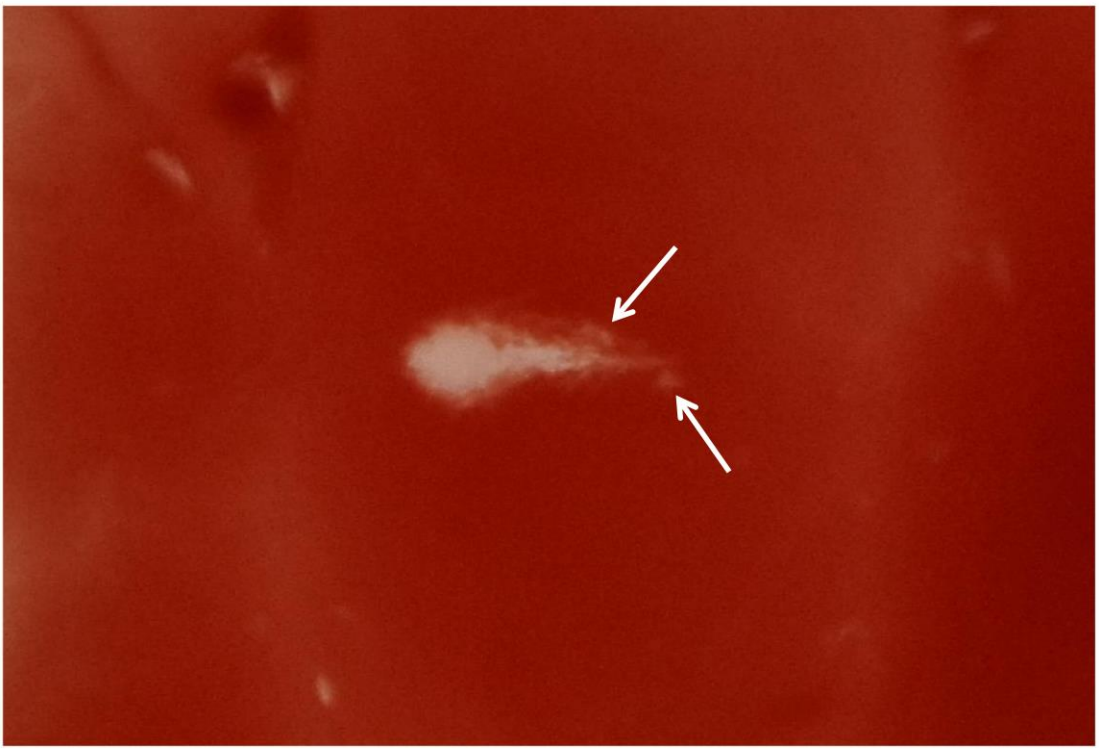

Figure S3: Gross digital photograph of liquefaction zone in a red blood cell phantom. The histotripsy pulse (1-MHz fundamental frequency, 5-μs pulse duration, 13-MPa peak negative pressure) propagated from left to right in the image. Discontinuous liquefaction regions along the periphery of the focal zone (white arrows) may indicate sites of persistent bubble clouds.